Journal of the Korean Society of Marine Engineering, Vol. 37, No. 3, pp. 274~281, 2013(ISSN 1226-9549)
http://dx.doi.org/10.5916/jkosme.2013.37.3.274

The influence of guide vane opening on the internal flow of a francis turbine

Qingsheng Wei[1] · Young-Do Choi†

(Received December 28, 2012 ; Revised March 6, 2013 ; Accepted April 25, 2013)

Abstract: The variable demand on the energy market requires a great flexibility in operating hydro turbines. However, Francis turbine operated at off-design conditions poses technical challenges related to large unsteady forces given by residual swirl and angular momentum. In order to improve the performance of a Francis turbine, the paper presents a numerical investigation of the 3D flow in the turbine at off-design conditions and discusses the influence of variable guide vane openings on the internal flow of a Francis turbine with the help of computational fluid dynamics. First, the internal flow characteristics of Francis turbine operated by varied guide vane angle at off design condition are computed and the optimal guide vane angle is obtained. Secondly, the Francis turbine is operated with guide vane number varies at the optimal guide vane angle. Finally, pressure contours and velocity distributions in the distributor are discussed and compared.

Keywords: Francis turbine, Guide vane opening, Internal flow, Performance

1. Introduction

Francis turbine is the most widely used turbine in the world. It has a wide head range from 20*m* to 700*m*. And its connected generator output power varies from just a few kilowatts up to one gigawatt. Besides, the most important fact is that its efficiency can be as high as over 90%.

However, guide vanes operated at off-design point resulting into the unsteady flow remains a challenge to overcome. Many studies were conducted experimentally and computationally to reveal and solve the problem. Hasmatuchi et al. **[1]** experimentally pointed out that pressure fluctuation in the turbine has some relations to the guide vane channels and the large vaneless space between the runner and the guide vane at low opening. Khare et al. **[2]** also proved that the guide vane opening have large influence in the whirl velocity at runner outlet by CFD method. Muntean et al. **[3][4]** monitored the cavitation performance of a Francis turbine operated at nominal head and variable discharge and obtained the proper guide vane axis location by simulating the 3-D flow characteristics for the whole operating range. Alnaga et al. **[5]** developed an automatic iterative procedure for optimal design of distributors(including stay vane and guide vane) and successfully applied in a Francis turbine.

However, the influence of guide vane for a certain Francis turbine is hard to standardized. In order to examine the influence of the guide vane opening to the internal flow of a Francis turbine with specific speed of 80.5, a series of CFD analysis are conducted in this study. First, CFD analysis on the internal flow of a Francis turbine model for up to 9 guide vane an-

† Corresponding author: Department of Mechanical Engineering, Mokpo National University, 1666 Youngsan-ro, Cheonggye-myeon, Muan-gun, Jeonnam 534-729, Republic of Korea, E-mail: ydchoi@mokpo.ac.kr, Tel: 061-450-2419
1 Department of Mechanical Engineering, Graduate School, Mokpo National University, E-mail: sidda306@126.com, Tel: 061-450-2419

gles is performed and an optimal guide vane angle is obtained. Secondly, CFD analysis on the turbine with guide vane number varying from 12 to 20 are conducted to get the ideal value. Finally, relations of the angle and number of guide vane with the performance of the turbine are examined using static pressure and circumferential velocity.

2. Turbine model

Figure 1 shows the schematic view of the Francis turbine model which is used for CFD analysis in this study. **Figure 1 (a)** shows the three dimensional view and **Figure 1 (b)** presents the two dimensional configuration of the turbine. The runner outlet diameter D_e is 0.350*m*. When the number of the blades is 17, the guide vane angle can be fully opened to 0.0694m(100%). The rotating speed of runner, effective head, output power and flow rate at the design point are N=900min^{-1}, H=60.73*m*, P=230*kW* and Q=0.46m^3/s, respectively.

Figure 2 (a) shows the 3D modeling of the guide vane. The guide vane rotates to the pivot to change the guide vane angle a_g as shown in **Figure 2 (b)**. Guide vane angle reaches its the maximum value of a_{gMAX}. When the tip of vane reaches the inlet of runner or inversely, it shows a less a_g. The area between guide vane and runner is defined as vaneless area.

Moreover, **Tables 1** and **2** show the cases of CFD analysis by the variation of guide vane angle and guide vane number. CFD analysis on the influence of guide vane angle is firstly carried out with guide vane number is 16 and optimal guide vane angle is obtained. Then CFD analysis on the influence of guide vane number is secondly conducted based on the optimal guide vane angle.

3. Numerical Methods

This study employs a commercial CFD code of ANSYS CFX **[6]** to conduct CFD analysis. As shown in **Figure 3**, tetrahedral numerical grids of about 19.8×10^6 are adopted for the analysis of the calculation domain including inlet pipe, casing, runner and draft tube. Relatively dense grids are applied to the runner. Fine hexahedral numerical grids are employed for the draft tube of the turbine.

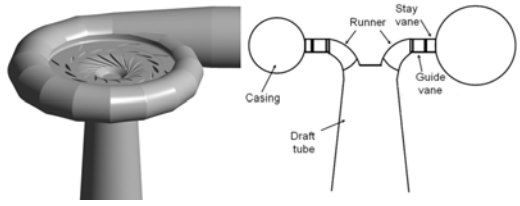

(a) (b)

Figure 1: (a) 3D view of Francis turbine model; (b) 2D view of Francis turbine model

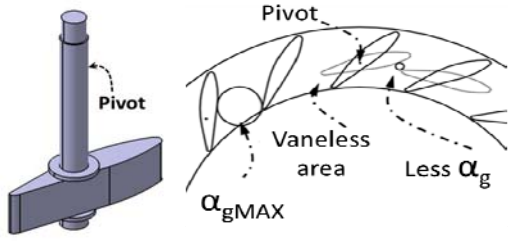

(a) (b)

Figure 2: (a) Guide vane modeling with pivot; (b) Schematic view of guide vane angle(a_g) variation

Table 1: Cases of CFD analysis by guide vane angle

Case	Guide vane angle [%]	Flow rate [$\times10^{-2}m^3/s$]
1	10.0	15.1
2	19.5	27.0
3	23.4	30.3
4	31.2	10.0
5	35.0	44.2
6 (design point)	38.9	46.0
7	46.7	56.6
8	50.6	59.9
9	54.5	62.6

Table 2: Cases of CFD analysis by guide vane number

Case	Guide vane number	Flow rate [$\times 10^{-2} m^3/s$]
Ⅰ	12	88.8
Ⅱ	14	62.5
Ⅲ (design point)	16	46.0
Ⅳ	18	35.0
Ⅴ	20	27.1

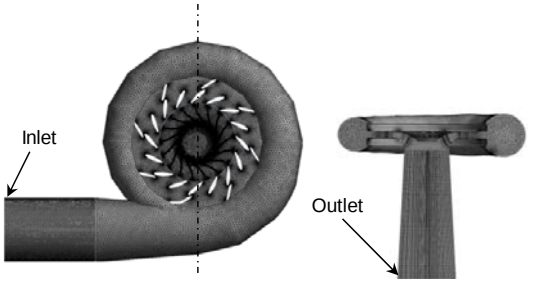

Figure 3: Numerical mesh of turbine model

Table 3: Numerical methods and boundary condition

Numerical methods	Mesh type	Tetra-hedral (turbine)& tetra-hedral (draft tube)
	Mesh number	19.8×10^6
	y^+	below 15(runner) below 50(casing)
	Turbulence model	*SST*
	Calculation type	Steady state
Boundary condition	Rotor-stator interface	Frozen rotor
	Inlet of turbine	Constant pressure
	Outlet of turbine	Averaged outflow
	Wall	No-slip

The numerical methods and boundary condition are set as shown in **Table 3**. Shear stress transport(*SST*) model is adopted as turbulence model because of its relatively good convergence in the complicated flow field of turbomachinery. The flow conditions are imposed at boundary conditions related to constant pressure estimated by ρgH at the inlet and averaged outflow at the outlet. At the interface between the rotating domain (runner) and stationary domain (guide vane & draft tube) a frozen-rotor interface is used. All calculations are conducted under the condition of steady state.

4. Results and Discussion

4.1 Performance curves

The flow field is investigated when guide vane openings (guide vane angle and guide vane number) are changed.

Figure 4 shows the performance curves of the Francis turbine model. The best efficiency point is taken as reference condition. As both guide vane angle and guide vane number are related to flow rate, flow rate ratios are considered to be the axis of abscissas and thus, the efficiency curves by two kinds of guide vane opening control methods can be easily compared. The axis of ordinates reveals normalized efficiency.

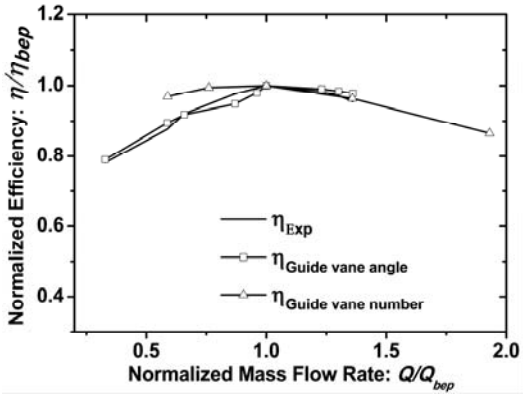

Figure 4: Efficiency curves by guide vane opening

The efficiency curve η_{EXP} is referred to the turbine manufacturer's design data **[7]**. The present CFD analysis result of efficiency curve by guide vane an-

gle presents a good convergence with the designed curve, which indicates that the adopted numerical method here is reliable.

Moreover, the CFD analysis result of efficiency curve by guide vane number shows a relatively better efficiency in partial load cases(Q/Q_{bep} is less than 1) but a little lower efficiency in excessive load cases in comparison with those by the results of guide vane angle control.

Compared with **Tables 1** and **2**, an optimal guide vane opening with guide vane angle opened to 38.9% and guide vane number equaled to 16 is obtained.

4.2 Pressure contours and velocity vectors by guide vane angle

Figure 5 shows the test plane and locations in the turbine. **Figure 5 (a)** shows the central plane for test pressure contours and velocity vectors because the data here are quite representative. **Figure 5 (b)** shows the six radial locations of pressure and velocity distributions on the plane. The inlet and outlet of guide vane, the vaneless area, the inlet, mid-radial and outlet of runner are noted as **Locations 1** to **6**.

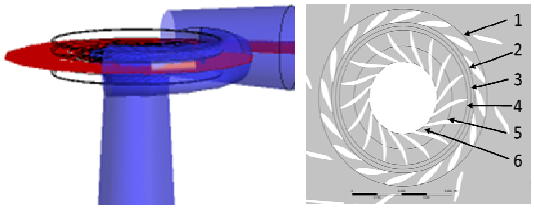

(a) (b)

Figure 5: (a) Test plane of pressure contours and velocity vectors; (b) Radial locations of pressure and velocity on the plane shown in **Figure 5 (a)**

Static pressure contours and velocity vectors in the turbine by guide vane angle are shown in **Figure 6**. Case 1 is chosen as representative for its typical internal flow characteristic of partial load case which is quite different from that of Case 6. Case 6 is a case by the flow rate at the best efficiency point(bep) that is considered as normal criterion. Similarly, Case 9 is chosen to present the internal flow characteristics of Francis turbine in over load condition.

Figure 6(a) shows a sharp pressure transition along the guide vane passages and lower pressure in the runner in Case 1 by partial load. On the contrary, pressure decreases gradually when water passes through relatively wide guide vane passages in Case 6.

Velocity vectors in **Figure 6 (b)** are taken from the same passage of the runner in **Figure 6 (a)**. Recirculation flow in the runner passage, which is shown as relative velocity vectors, and relatively high circumferential velocity, which is shown as absolute velocity vectors, in the vaneless area are observed in Case 1, which could be the reasons that the efficiency of Case 1 is quite lower than that of Case 6.

On the other hand, the velocity vectors in Case 9 show a quite uniform flow passing through the runner passage.

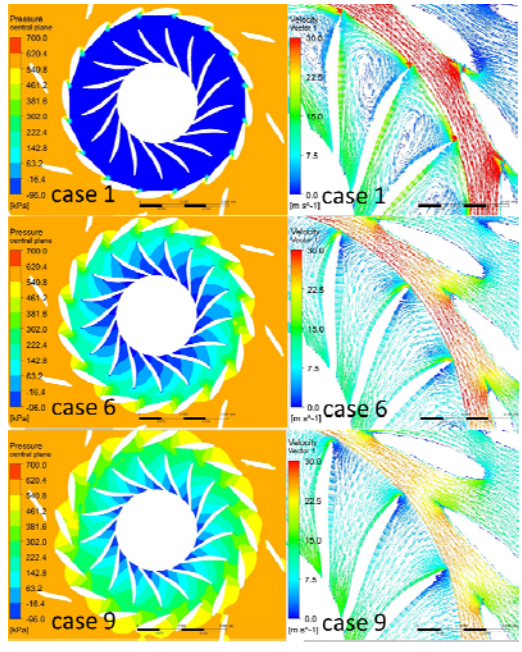

(a) Pressure contours (b) Velocity vectors

Figure 6: Pressure contours and velocity vectors in the turbine by guide vane angle.

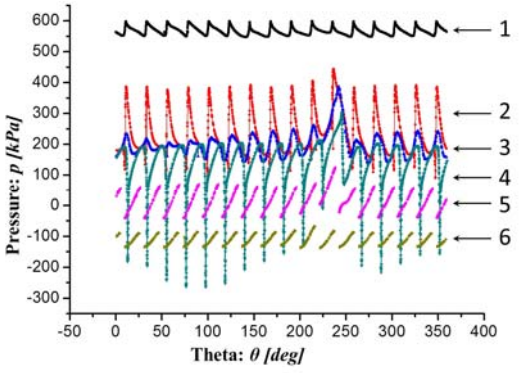

Figure 7: Pressure distributions in the turbine at the design point (Case 6).

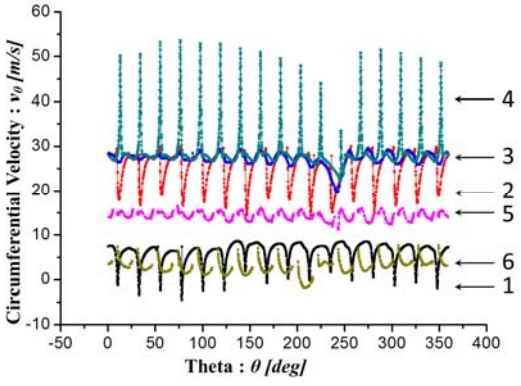

Figure 8: Absolute circumferential velocity distributions in the turbine at the design point (Case 6).

Figures 7 and **8** show the static pressure and absolute circumferential velocity distributions from **Locations 1** to **6** at the designed flow rate range of Case 6. The test locations are shown in the **Figure 5**.

The pressure distributions at each location show gradual decrease of static pressure from **Locations 1** to **6**. The decreased static pressure changes to output torque in the runner passage.

Moreover, circumferential velocity distributions show that, from **Locations 1** to **3**, the velocity increases gradually due to the guided flow direction by the guide vane but decreases apparently from **Locations 4** to **6**, which means that the increased angular momentum in the regions from **Locations 1** to **4** changes to output torque in the **Locations 4** to **6**.

Figure 9 shows the pressure distributions in the Francis turbine by the differential pressure coefficient:

$$\triangle C_p = \frac{2(p_{in} - p)}{\rho(R\omega)^2} \quad (1)$$

where p_{in} is the static pressure at the inlet of turbine casing and p is the local static pressure of test location, R is the diameter of runner inlet, and ω is angular velocity.

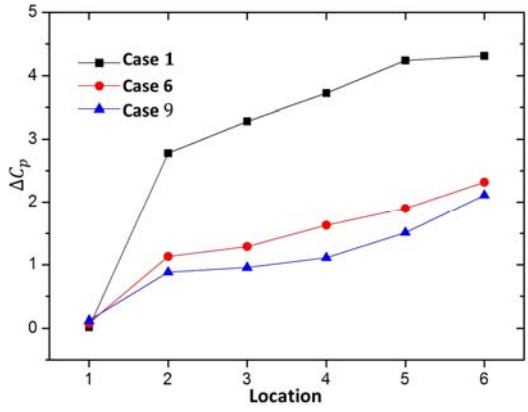

Figure 9: Averaged pressure distributions in the turbine by guide vane angle.

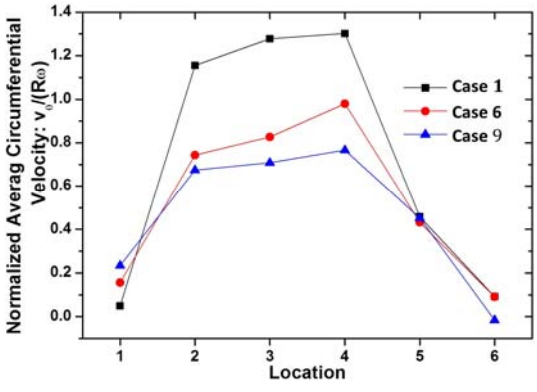

Figure 10: Averaged circumferential velocity distributions in the turbine by guide vane angle.

The difference of static pressure increases drastically between the **Locations 1** and **2** in all case as shown in **Figure 9**, which implies that pressure decrease occurs considerably at the guide vane passage because of the increased circumferential velocity in the guide vane passage. Especially, in the Case 1, the amount of pressure decrease is considerably larger than those of the other cases. The larger amount of pressure decrease at the guide vane passage may lead to the low efficiency in the partial load ranges.

Figure 10 shows the averaged circumferential velocity distributions in those three cases. Case 1 shows relatively higher velocity from **Locations 2** to **4** but decrease drastically from **Locations 4** to **5**, which means that there exists considerable hydraulic loss by recirculation flow in the runner passage as shown in **Figure 6 (b)**.

4.3 Pressure contours and velocity vectors by guide vane number

Corresponding to the flow rate in Case 1, Case 6 and Case 9, Case Ⅳ, Case Ⅲ and Case Ⅱ are chosen as typical cases to analyse to internal flow characteristics in the Francis turbine influenced by the guide vane number, respectively. **Figure 11** shows the pressure contours and velocity vectors on the test plane shown in **Figure 5 (a)** by guide vane number. Unlike the cases by guide vane angle, the less of guide vane number is, the larger the guide vane opening will be. As the guide vane angle and inlet pressure are set to same value in all cases, and Case Ⅱ has the largest flow rate, static pressure at the runner passage in Case Ⅱ is lower than those of the other cases as shown in **Figure 11 (a)**.

On the other hand, Unlike the velocity vectors of Case 1 in **Figure 6 (b)**, there is no recirculation flow region in the runner passage even at the partial load condition in Case Ⅳ. Relatively higher guide vane angle in Case Ⅳ than that of Case 1 should have lead the main stream of the flow into the runner passage without the occurrence of recirculation flow.

Figure 12 shows the averaged pressure distributions by the differential pressure coefficient $\triangle C_p$ in the Francis turbine model according to the variation of guide vane number. Case Ⅱ shows relatively higher value of $\triangle C_p$ at all locations in comparison with those of Cases Ⅲ and Case Ⅳ. The tendency of pressure distribution in the turbine passage by the guide vane number is close to proportional to the flow rate by comparing the $\triangle C_p$ versus to test location curves of Case Ⅱ, Cases Ⅲ and Case Ⅳ.

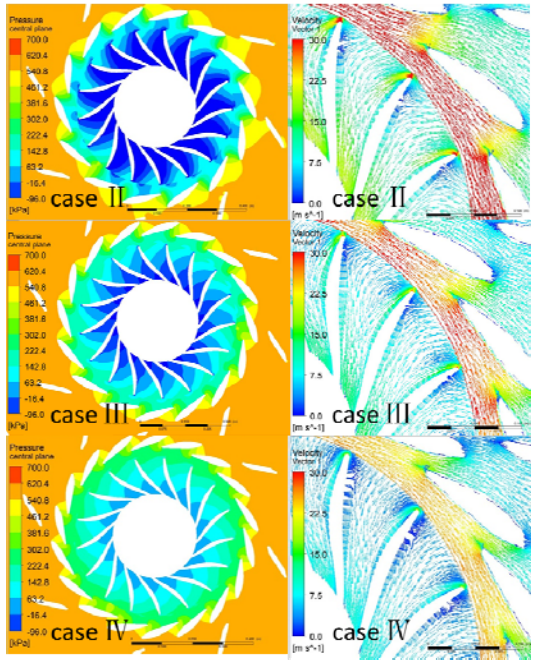

(a) Pressure contours (b) Velocity vectors

Figure 11: Pressure contours and velocity vectors in the turbine by guide vane number.

Figure 13 shows the averaged circumferential velocity distributions in the turbine by guide vane number. Due to the same guide vane angle, circum-

ferential velocity at the **Locations 1** to **4** shows almost same distribution pattern with the change of the velocity at each location according to the mass flow rate of the Cases Ⅱ to Ⅳ. And then, the circumferential velocity decrease abruptly from the **Locations 4** to **6**.

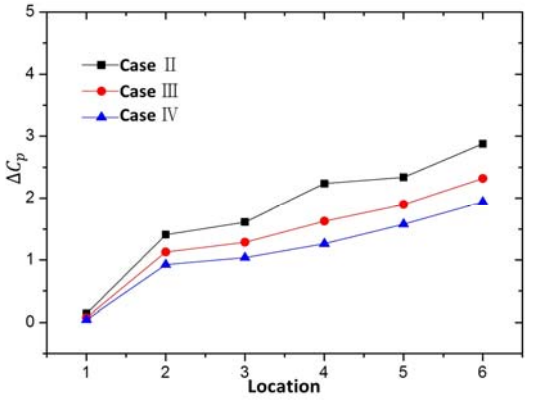

Figure 12: Averaged pressure distributions in the turbine by guide vane number.

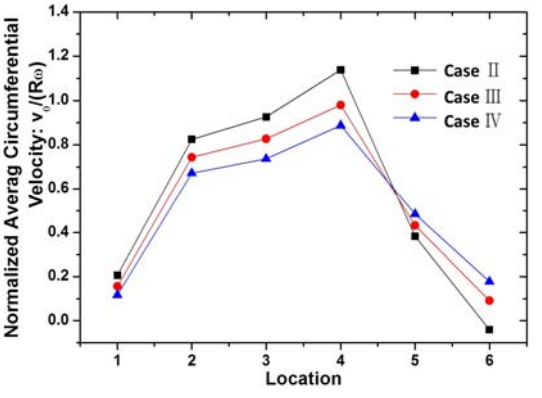

Figure 13: Averaged circumferential velocity distributions in the turbine by guide vane number.

5. Conclusions

According to the investigation of the influence of guide vane opening, which includes the variation of angle and number of the guide vane, guide vane opening gives considerable influence to the internal flow and performance of the Francis turbine. The optimum guide vane opening is obtained at a guide vane angle of 38.9% and at a guide vane number16. Relatively larger variation of the pressure and velocity distributions is found by guide vane angle in comparison with that of guide vane number. Guide vane opening controlled by guide vane number shows a quite better efficiency in partial load condition than that by guide vane angle, other than almost equivalent efficiency in excessive load condition. More uniform flow in the turbine runner passage occurs in partial load cases by guide vane number. Therefore, in order to get a larger operating range, a possible way to is to control the mass flow rate with the guide vane number by keeping the guide vane angle.

Acknowledgements

This research was financially supported by the Ministry of Education, Science and Technology (MEST) and National Research Foundation of Korea(NRF) and Jeonnam Science & Technology Promotion Center (JNSP) through the research & development project of Jeonnam Science Park.

Reference

[1] V. Hasmatuchi, M. Farhat, P. Maruzewski, and F. Avellan, "Experimental investigation of a pump-turbine at off-design operating conditions," Proceedings of the 3rd International Association for Hydro-Environment Engineering and Research International Meeting of the Workgroup on Cavitation and Dynamic Problems in Hydraulic Machinery and Systems, pp. 339-347, 2009.

[2] R. Khare, V. Prasad, and S. Kumar, "CFD approach for flow characteristics of hydraulics Francis turbine," International Journal of Engineering Science and Technology, vol. 2, no. 8, pp. 3824-3831, 2010.

[3] S. Muntean, R. F. Susan-Resiga, S. Bernad, and I. Anton, "Analysis of the GAMM Francis tur-

bine distributor 3D flow for the whole operating range and optimization of the guide vane axis location," Proceedings of the 6th International Conference on Hydraulic Machinery and Hydrodynamics, pp. 131-136, 2004.

[4] S. Muntean, I. Ninaci, R. Susan-Resiga, A. Baya, and I. Anton, "Numerical analysis of the flow in the old Francis runner in order to define the refurbishment strategy," University Politehnica of Bucharest Scientific Bulletin, Series D, vol. 72, no. 1, pp. 117-124, 2010.

[5] A. Alnaga and J. L. Kueny, " Optimal design of hydraulic turbine distributor," World Scientific and Engineering Academy and Society Transactions on Fluid Mechanics, vol. 3, no. 2, pp. 175-185, 2008.

[6] ANSYS CFX Documentation, http://www.ansys.com, Accessed May 20, 2012.

[7] Tanaka Suiryoku, Technical Design Book of Francis Hydro Turbine, Japan, 2012.